

Polymerization in the Gas Phase, in Clusters, and on Nanoparticle Surfaces

M. SAMY EL-SHALL

Department of Chemistry, Virginia Commonwealth University,
Richmond, Virginia 23284-2006

RECEIVED ON JUNE 9, 2007

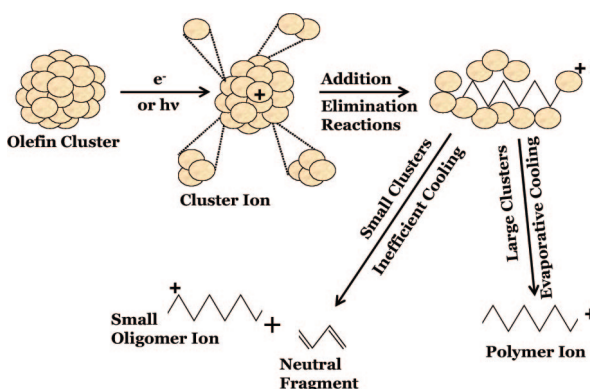
CON SPECTUS

Gas phase and cluster experiments provide unique opportunities to quantitatively study the effects of initiators, solvents, chain transfer agents, and inhibitors on the mechanisms of polymerization. Furthermore, a number of important phenomena, unique structures, and novel properties may exist during gas-phase and cluster polymerization. In this regime, the structure of the growing polymer may change dramatically and the rate coefficient may vary significantly upon the addition of a single molecule of the monomer. These changes would be reflected in the properties of the oligomers deposited from the gas phase.

At low pressures, cationic and radical cationic polymerizations may proceed in the gas phase through elimination reactions. In the same systems at high pressure, however, the ionic intermediates may be stabilized, and addition without elimination may occur. In isolated van der Waals clusters of monomer molecules, sequential polymerization with several condensation steps can occur on a time scale of a few microseconds following the ionization of the gas-phase cluster. The cluster reactions, which bridge gas-phase and condensed-phase chemistry, allow examination of the effects of controlled states of aggregation.

This Account describes several examples of gas-phase and cluster polymerization studies where the most significant results can be summarized as follows: (1) The carbocation polymerization of isobutene shows slower rates with increasing polymerization steps resulting from entropy barriers, which could explain the need for low temperatures for the efficient propagation of high molecular weight polymers. (2) Radical cation polymerization of propene can be initiated by partial charge transfer from an ionized aromatic molecule such as benzene coupled with covalent condensation of the associated propene molecules. This novel mechanism leads exclusively to the formation of propene oligomer ions and avoids other competitive products. (3) Structural information on the oligomers formed by gas-phase polymerization can be obtained using the mass-selected ion mobility technique where the measured collision cross-sections of the selected oligomer ions and collision-induced dissociation can provide fairly accurate structural identifications. The identification of the structures of the dimers and trimers formed in the gas-phase thermal polymerization of styrene confirms that the polymerization proceeds according to the Mayo mechanism. Similarly, the ion mobility technique has been utilized to confirm the formation of benzene cations by intracuster polymerization following the ionization of acetylene clusters. Finally, it has been shown that polymerization of styrene vapor on the surface of activated nanoparticles can lead to the incorporation of a variety of metal and metal oxide nanoparticles within polystyrene films.

The ability to probe the reactivity and structure of the small growing oligomers in the gas phase can provide fundamental insight into mechanisms of polymerization that are difficult to obtain from condensed-phase studies. These experiments are also important for understanding the growth mechanisms of complex organics in flames, combustion processes, interstellar clouds, and solar nebula where gas-phase reactions, cluster polymerization, and surface catalysis on dust nanoparticles represent the major synthetic pathways. This research can lead to the discovery of novel initiation mechanisms and reaction pathways with applications in the synthesis of oligomers and nanocomposites with unique and improved properties.



1. Introduction

Most of the current knowledge of polymerization reactions and polymer properties comes from experiments dealing with bulk liquids or solutions.^{1–4} This is because these are the preferred media for many industrial and laboratory polymerization processes. However, a number of important phenomena, unique structures, and novel properties may exist for gas-phase and cluster polymerization.^{5–48} In this regime, the structure of the growing polymer may change dramatically and the rate coefficient may vary significantly upon the addition of a single monomer molecule. These changes would be reflected in the properties of the oligomers. Gas phase and cluster studies can provide unique opportunities to quantitatively study the effects of solvents, charge transfer, and inhibitors on the mechanisms of polymerization. The combination of structural information on the growing oligomers and on bulk polymers can provide detailed understanding of the *structure–property* relationship in polymer systems.

From a practical point of view, gas-phase and cluster polymerization can lead to the synthesis of defect-free, uniform thin polymeric films of controlled morphology and tailored compositions for many technological applications such as protective coatings and electrical insulators. For example, the polymeric species could be deposited from the gas phase in a size-selected manner on metal or semiconductor surfaces. Furthermore, gas-phase polymerization can be coupled with the vapor phase synthesis of metal and semiconductor nanoparticles to generate novel hybrid materials, which combine several properties such as strength, elasticity, electrical conductivity and improved electro-optic performance.

The ion chemistry of olefin, diolefin, alkyne, and conjugated molecules plays an important role in the gas-phase polymerization process.^{5,49–52} These monomers can be induced to oligomerize or polymerize through bimolecular ion–molecule reactions in the gas phase.^{49–52} The reactions can be initiated by an appropriate cation or radical cation, which can transfer the charge to the selected monomer molecule. In the gas phase at low pressures, cationic polymerization may proceed via elimination reactions.^{5,49–52} However, in the same systems at high pressure, the ionic intermediates may be stabilized and addition without elimination may occur. In isolated van der Waals (vdW) clusters of monomer molecules, both elimination and addition polymerization can take place resulting in a product ion distribution that reflects the stability of the polymeric ions and the kinetics of the reaction.^{8–11,13–15} The competition between the condensation reactions leading to the growth of the oligomer ion and

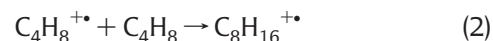
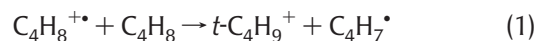
monomer evaporation resulting in depletion of the monomer concentration in the cluster can control the ultimate size that the oligomer ion can reach in the cluster.

Intracluster ionic polymerization was first demonstrated in our laboratory^{8,9} and is currently becoming an active area of research. Several groups have developed laser and mass spectrometric methods to study anionic, cationic, and metal ion-induced intracluster polymerization.^{8–11,13–15,20–25,29,31,34–37,40–42,44,46} Other groups have developed novel approaches to determine the gas-phase conformations of a variety of oligomers and polymers including biopolymers, synthetic polymers, metal ion cationized polymers, and photoluminescence-conjugated polymers.^{53–61} Our group has focused on studying the early stages of cationic and radical cation polymerization within clusters of a variety of unsaturated organic molecules.^{8,9,15,18,22–25,28,29,34,41,42,44,46} In this Account, we describe several examples of gas-phase and cluster polymerization studies with special emphasis on understanding the reaction mechanisms, the structural identification of oligomers formed in the early stages of polymerization and the incorporation of nanoparticles within polymeric materials formed by gas-phase processes.

2. Gas-Phase Polymerization of Olefin Radical Cations

Isobutene is one of the few monomers known to be polymerized exclusively by cationic mechanisms.⁴ Although it is generally accepted that high molecular weight polyisobutylene is formed through the propagation of the *t*-butyl cation ($t\text{-C}_4\text{H}_9^+$), the exact nature of the mechanism and the contributions from the reactions of the radical cation $\text{C}_4\text{H}_8^{+\bullet}$ have never been clearly elucidated from the condensed-phase studies.^{1,4}

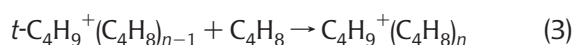
Carbocation vs Radical Cation Polymerization. Gas-phase reactions of isobutene after ionization follow two typical paths, radical ion chemistry (of C_4H_8^+ and its products, eq 1) and carbocation chemistry (of $t\text{-C}_4\text{H}_9^+$ and its products, eq 2).²⁴



High-pressure mass spectrometry (HPMS) results showed that the dimer is a covalent adduct with a dissociation energy >132 kJ/mol, which is significantly larger than typical binding energies of noncovalent ion–molecule complexes.²⁴ Through charge transfer bracketing, the dimer was identified as the ion generated from a branched octene with an ioniza-

tion energy (IE) of 8.55 ± 0.15 eV. The most likely structure of the dimer cation is $(\text{CH}_3)_2\text{CHCHCHCH}(\text{CH}_3)_2^{+\bullet}$, which could be produced by sterically favorable tail-to-tail addition of the C_4H_8^+ ion to the isobutene molecule. This structure can be formed by two hydrogen shifts in the initially formed condensation product $(\text{CH}_3)_2\text{C}^+\text{CH}_2\text{CH}_2\text{C}^*(\text{CH}_3)_2$ in which both the ionic and radical sites are stabilized on tertiary carbons.

In the carbocation branch, the addition reaction (eq 3) for $n = 1$, was found to be reversible at 230–400 K, with $\Delta H^\circ = -95.8$ kJ/mol and $\Delta S^\circ = -136.8$ J/(mol K).²⁴



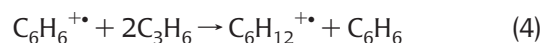
Of particular interest is the second polymerization step, $n = 2$ in reaction 3, which showed an unusually large thermochemical change, with $\Delta H^\circ = -101.3$ kJ/mol and $\Delta S^\circ = -203.7$ J/(mol K).²⁴ The large entropy change is characteristic of sterically hindered reactions.⁵ Parallel to the thermochemistry, the kinetics of the second step also showed an anomaly. While the reaction efficiency of the first step was near unity, the second step was slower by orders of magnitude, with a reaction efficiency of 0.005 and with a large negative temperature coefficient of $T^{-1.6}$. The third and fourth steps are still slower but with smaller temperature coefficients. Slower rates and large negative temperature coefficients of the second polymerization step are characteristic of reactions about sterically hindered centers and result from entropy barriers due to the freezing of internal rotors in the transition state.^{5,24}

A remarkable consistency with the gas-phase kinetics and thermochemistry data is observed in the clusters' study.²⁵ We generated clusters in a supersonic beam expansion of isobutene or of benzene/isobutene mixtures, followed by electron impact or multiphoton ionization.²⁵ In both the pure and mixed clusters, species containing the isobutene dimer cation ($\text{C}_8\text{H}_{16}^{+\bullet}$) are enhanced, suggesting a stable covalent adduct, consistent with the gas-phase results. The cluster results indicate that the formation of the dimer cation is more favorable than that of the carbocation under the cold beam conditions.²⁵ Also, the decrease of the $t\text{-C}_4\text{H}_9^+$ condensation channel with increasing cluster size, where energy dissipated to the cluster modes becomes more efficient, is consistent with the gas-phase temperature dependence of the isobutene ion chemistry.

Initiation of Radical Cation Polymerization by Coupled Charge Transfer—Covalent Condensation. In the benzene/isobutene system, we observed that fast thermoneutral charge transfer from the aromatic to the olefin initiates polymeriza-

tion.^{24,25} This occurs because the IE of benzene is higher than that of isobutylene (IE = 9.239 eV);²⁴ therefore, direct charge transfer from benzene⁺ to isobutylene generates the $\text{C}_4\text{H}_8^{+\bullet}$ ion, which then undergoes the competitive proton transfer or the dimerization reactions to generate the $t\text{-C}_4\text{H}_9^+$ and $\text{C}_8\text{H}_{16}^{+\bullet}$ ions, respectively. We wondered about a system where charge transfer to the olefin monomer would be prohibitively endothermic but would lead to a dimer with lower ionization energy than the aromatic. Could the two olefin molecules act as a charge receptor to form a product with a low IE, leading to an overall exothermic reaction?^{38,45}

In the benzene cation/propene system, the aromatic initiator (C_6H_6) has an IE between the reactant's monomer (C_3H_6) and its covalent dimer (C_6H_{12}), that is, $\text{IE}(\text{C}_3\text{H}_6) > \text{IE}(\text{C}_6\text{H}_6) > \text{IE}(\text{C}_6\text{H}_{12})$.³⁸ Therefore, direct charge transfer from $\text{C}_6\text{H}_6^{+\bullet}$ to C_3H_6 is not observed due to the large endothermicity of 0.48 eV, and only the adduct $\text{C}_6\text{H}_6^{+\bullet}(\text{C}_3\text{H}_6)$ is formed. However, coupled reactions of charge transfer with covalent condensation involving the $\text{C}_6\text{H}_6^{+\bullet}$ ion and two C_3H_6 molecules are observed according to the overall process:



Reaction 4 represents an initiation mechanism for the gas-phase polymerization of propene since it results in the formation of the dimer radical cation ($\text{C}_6\text{H}_{12}^{+\bullet}$), which can sequentially add several propene molecules. At higher concentrations of propene, the reaction products are the propene oligomers (C_3H_6)_{*n*}⁺ with $n = 2-7$ and the adduct series $\text{C}_6\text{H}_6^{+\bullet}(\text{C}_3\text{H}_6)_n$ with $n \leq 6$. Figure 1a displays the time profiles corresponding to the sequential generation of the (C_3H_6)_{*n*}⁺ series with n up to 5 (denoted as P_2 , P_3 , P_4 , and P_5). Figure 1b shows the normalized time profiles corresponding to the disappearance of the $\text{C}_6\text{H}_6^{+\bullet}$ ion signal (B), and the appearance of the two parallel channels $\text{C}_6\text{H}_6^{+\bullet}(\text{C}_3\text{H}_6)_m$ with $m=1-3$ (ΣBP_m), and the (C_3H_6)_{*n*}⁺ series with $n = 2-6$ (ΣP_n). The significance of the coupled charge transfer/covalent condensation reactions is that the overall process leads exclusively to the formation of condensation products (C_3H_6)_{*n*}⁺ and avoids other competitive channels in the ion–molecule reactions of propene.³⁸

The basic mechanism of charge transfer coupled with covalent condensation has been confirmed by using both the selected ion flow tube (SIFT) and the mass-selected ion mobility (MSIM) techniques.^{38,45} The results suggest that a similar mechanism may actually be operative in solution. Since benzene and toluene are often used as polymerization solvents, this may open the possibility for a "solvent as initiator

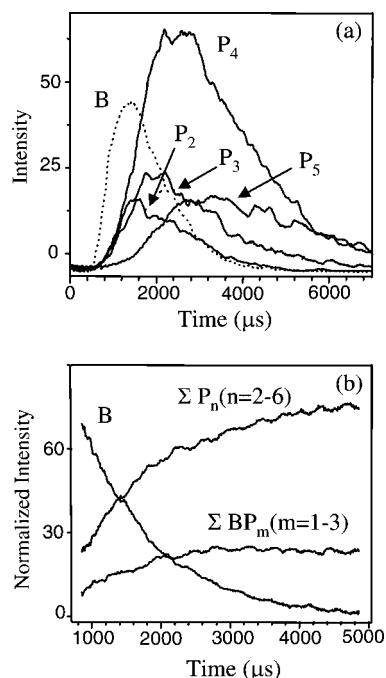


FIGURE 1. (a) Raw ion time profiles (P_2 , P_3 , P_4 , and P_5 represent $(C_3H_6)_n^{++}$ series with n up to 5) and (b) normalized time profiles due to reactant (benzene $^{++}$, B) and products (P_n with $n = 2-6$ and BP_m with $n = 1-3$) in the benzene $^{++}$ /propene.

approach", which would eliminate the need for chemical initiators or additives.

3. Structures of Thermally Polymerized Styrene Oligomers

The mechanism of the self-initiated polymerization (or thermal polymerization) of styrene in bulk liquids or solutions has been a challenging subject of research since the early days of polymer chemistry.^{1,62} The Mayo mechanism (Figure 2) is the most generally accepted mechanism for the spontaneous polymerization of styrene.⁶³⁻⁶⁵ It proceeds via Diels-Alder dimerization to produce the transient dimer **1**, which reacts with styrene to generate radicals **I** and **II**. These radicals start the styrene propagation, couple to form trimer **3**, and disproportionate to form dimer **2-a** and styrene. The addition of styrene to radical **I** produces a dimer, which can be terminated by chain transfer to form **2-b**, or add further styrene molecules to form polymers. A recent theoretical study supports polymerization via **1** but shows that **1** is formed by a stepwise, not a concerted, reaction.⁶⁶

We applied the MSIM technique to gain new insights on the mechanism of gas-phase thermal polymerization of styrene.⁴² The MSIM technique has been developed by Bowers and Jarrold to provide structural information on a variety of clusters including carbon, metal, and mixed metal carbon clus-

ters, as well as polymers, host-guest pairs, and biological molecules in the gas phase.⁵³⁻⁶¹ Structural information on the ionized clusters and oligomers are obtained by measuring the average collision cross-section (Ω) of the mass-selected ion with an inert buffer gas such as helium.^{67,68} Theoretical calculations of possible structural candidates of the mass-selected ion are then used to compute angle-averaged Ω 's at different temperatures for comparison with the measured ones. Furthermore, collisional-induced dissociation (CID) of the mass-selected ions provides further support for the structures obtained from the mobility measurements.⁴²

In the experiments to study the gas-phase thermal polymerization of styrene (see Figure 3a), the styrene-helium vapor mixture is heated to well-defined temperatures (350-370 K) in order to generate oligomers in the vapor phase by thermal initiation. The vapor mixture is then expanded into vacuum through a supersonic pulsed nozzle thus resulting in an adiabatic cooling of the vapor and quenching of the polymerization process. The clusters (oligomers + monomers) are then ionized by EI, mass-selected through a quadrupole mass filter, and injected into a drift cell containing helium buffer gas. Both the ionization and ion injection processes lead to extensive evaporation of the nonreacted styrene monomers, thus leaving only the thermalized bare oligomer ions to travel through the drift cell. Figure 3b displays an example of the mass spectrum of the styrene oligomer ions obtained after traveling through the drift cell containing 1.2 Torr of He buffer gas. For the mobility measurements, ions exiting the cell are mass-analyzed and collected as a function of time yielding the arrival time distributions (ATDs) from which the mobilities and Ω 's in helium are determined.^{42,67,68}

The ATDs of the styrene dimer cation are shown in Figure 4. The significant broadening of the ATDs observed at higher temperatures suggests that different styrene dimers are present. The mobility measurements of the dimer yield average Ω 's of 108 ± 3 , 92 ± 3 , and $90 \pm 4 \text{ \AA}^2$ at 125, 303, and 453 K, respectively.⁴² Using DFT calculations at the B3LYP/6-31G** level, we obtained lowest energy structures of several styrene dimer radical cation isomers (12 most likely isomers were considered including the styrene ion-molecule head-to-tail and head-to-head parallel structures, *cis*- and *trans*-1,2 diphenylcyclobutanes, 1-methyl, 3-phenylindane, and structures **2-a** and **2-b**).⁴² The DFT lowest energy structure of the dimer cation (structure **D-a** corresponding to the neutral **2-a**) results in an average Ω of 107 \AA^2 at 125 K. The DFT second and third lowest energy structures (**D-b** and **D-c**, respectively) result in average Ω 's of 90.3 \AA^2 at 303 K and 90 \AA^2 at 453 K, respectively. It is clear that the dimer structures **D-a**, **D-b**,

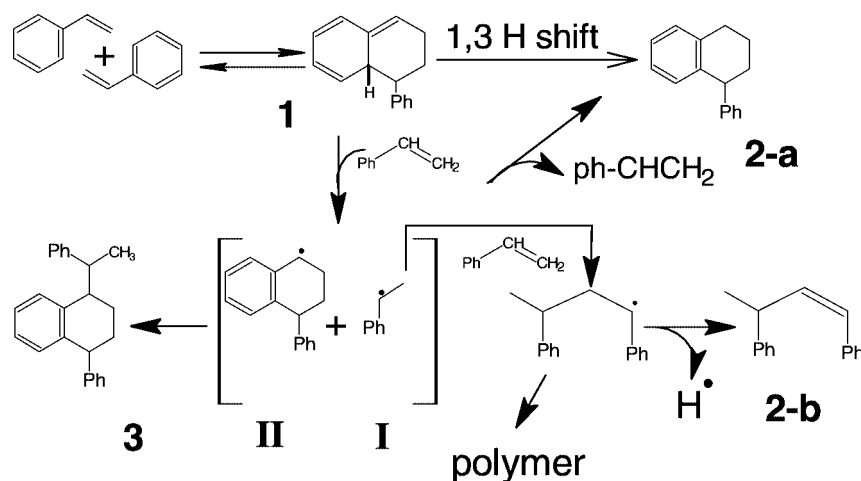


FIGURE 2. Illustration of the Mayo mechanism for the self-initiated polymerization of styrene.

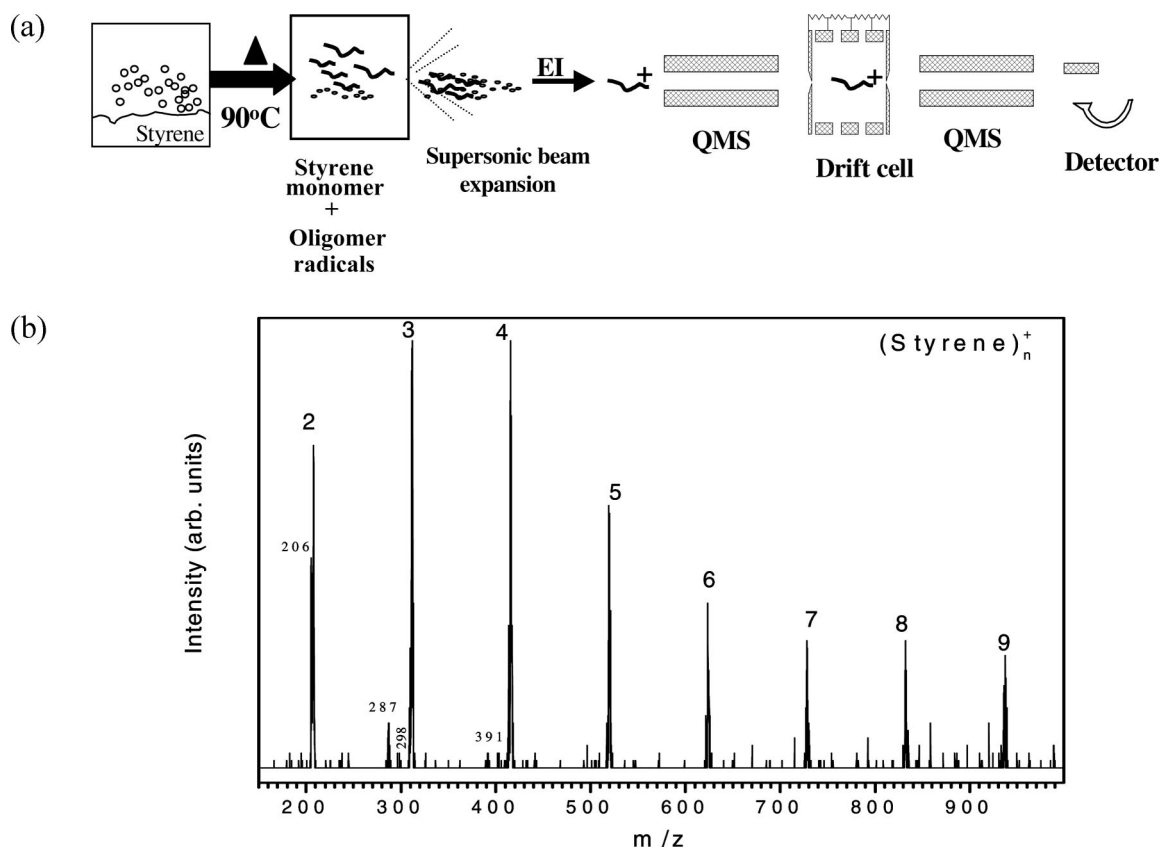


FIGURE 3. (a) Schematic diagram of the experimental approach used to study the gas-phase thermal polymerization of styrene using the mass-selected ion mobility technique and (b) mass spectrum of styrene oligomer ions, $(C_8H_8)_n^+$, obtained following their travel through the drift cell containing 1.2 Torr He.

and **D-c** (Figure 5) provide Ω 's in excellent agreement with the experimental values at the temperatures of 125, 303, and 453 K, respectively. By variation of the relative abundances of structures **D-a**, **D-b**, and **D-c**, excellent fits to the measured ATDs can be obtained at different temperatures as shown in Figure 4.⁴²

The neutral dimers corresponding to the cations **D-a** and **D-c** can be formed by the radical reactions as shown in the

Mayo's mechanism while the dimer cation **D-b** is formed by a cationic mechanism. In fact, previous work identified the dimer cation **D-b** as the covalent dimer formed in the gas-phase and intracuster reactions of styrene radical cation with its neutral molecule.²⁹ Therefore, the dimer **D-b** could be formed in our experiment following the EI ionization of the neutral styrene clusters generated by the beam expansion. Further evidence supporting structures **D-a** and **D-c** comes

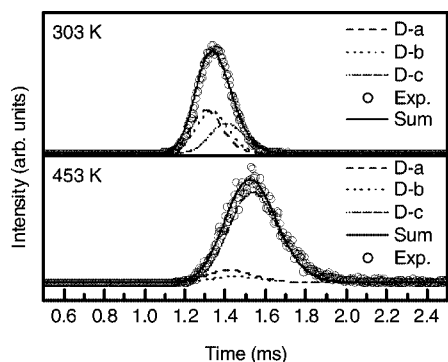


FIGURE 4. Arrival time distributions (ATDs) of mass-selected styrene dimer ion obtained at two temperatures (○) and theoretical fits (—) of the ATDs using the three structures **D-a**, **D-b**, and **D-c** shown in Figure 5.

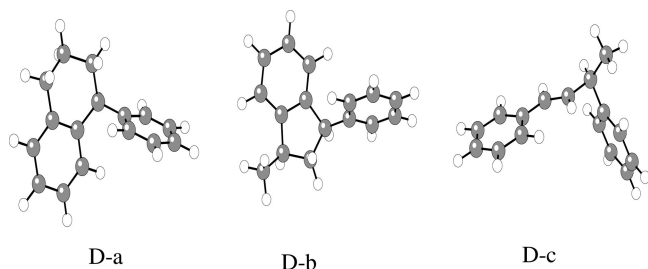


FIGURE 5. Structures used to reproduce the measured ATDs of the styrene dimer ion.

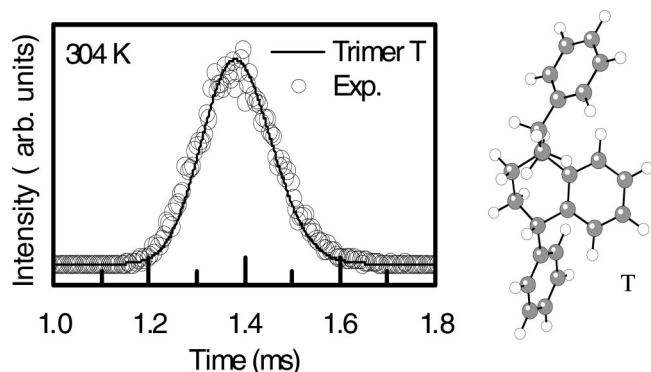


FIGURE 6. ATD of the styrene trimer cation at 304 K and the calculated lowest energy structure **T** providing excellent fit (—) to the measured ATD (○).

from the CID results. The mass-selected dimer ion shows fragmentation by the loss of a C_6H_6 unit consistent with structure **D-a**. In addition, the observed loss of a CH_3 group is consistent with isomer **D-c**. Thus, the correlations between calculated and experimental ATD values and the CID results allow us to determine that gas-phase thermal polymerization of styrene results in dimers **2-a** and **2-b**, consistent with an initiation process that proceeds according to Mayo mechanism (Figure 2).

Figure 6 displays the measured ATD of the mass-selected styrene trimer cation at 304 K and the calculated trimer structure **T** (corresponding to the neutral **3** in Figure 2). The exper-

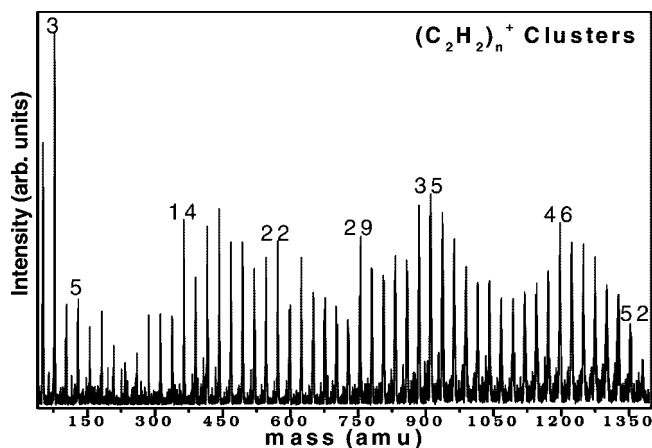


FIGURE 7. Mass spectrum of EI ionized acetylene clusters.

imental Ω for the trimer ($118 \pm 4 \text{ \AA}^2$) is in excellent agreement with the calculated Ω of structure **T** (119 \AA^2).⁴² It is interesting that the structure of the gas-phase trimer **T** is identical to the structure of the trimer isolated by HPLC from the thermal polymerization of styrene in solution and characterized by NMR.⁶⁴ The observation of the abundant trimer **T** (Figure 3b) is consistent with the recent theoretical predictions, which indicate that the barrier to the formation of **3** is lower than the barrier to generate the two benzylic monoradicals **I** and **II**.⁶⁶ The ion mobility results provide direct evidence for the trimer formation by recombination of the initially formed initiating radicals **I** and **II**.⁴²

The similarity between the initiation mechanism of the thermal polymerization of styrene in the gas phase and in bulk liquid or solution is remarkable and *implies* that the structures of the early oligomers in the gas phase are relevant to the understanding of the polymerization mechanisms in condensed phases. This is a significant result because it allows oligomer structures generated by different initiation mechanisms to be quickly and reliably determined using the ion mobility approach.

4. Polymerization of Ionized Acetylene Clusters

It has been postulated that benzene is the “missing link” between simple carbon molecules and the complex molecules made of hundreds of carbon atoms that could be responsible for the unidentified infrared bands.^{69,70} We used a combination of MSIM, CID, hydration energy measurements, and theoretical calculations to provide the most conclusive evidence for the formation of benzene ions from ionized acetylene clusters.^{46,48}

Figure 7 displays a typical mass spectrum obtained by EI ionization of neutral acetylene clusters formed by supersonic

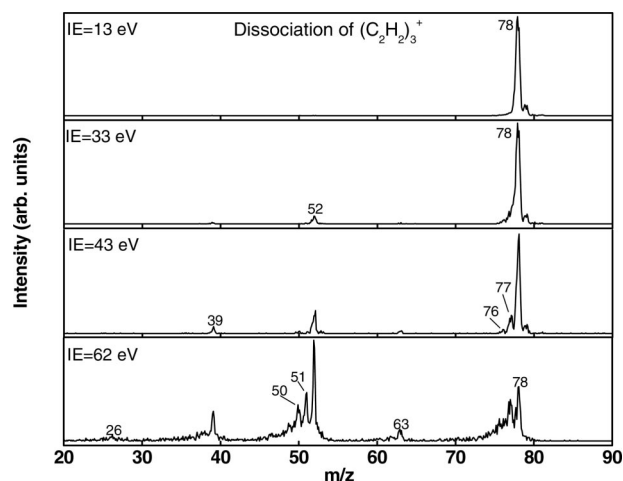


FIGURE 8. Dissociation of the mass-selected $(\text{C}_2\text{H}_2)_3^+$ ions by increasing the injection energies into the drift cell.

beam expansion. The distribution of the cluster ions formed reveals some striking features corresponding to the enhanced intensities (magic numbers) for the $(\text{C}_2\text{H}_2)_n^+$ with $n = 3, 14, 22, 29, 35,$ and 46 .

The strong magic number at $n = 3$ is consistent with the formation of a stable C_6H_6^+ ion in an exothermic process that can lead to extensive evaporation of neutral acetylene molecules from the cluster as indicated by the depletion of the ion signal corresponding to $n = 4-10$. The stability of the $(\text{C}_2\text{H}_2)_3^+$ ion is demonstrated in Figure 8. No fragmentation is observed when injection energy of 13 eV is used, and very little fragmentation occurs when using an injection energy of 33 eV. At an injection energy of 62 eV, the observed fragments from the $(\text{C}_2\text{H}_2)_3^+$ ion are C_6H_5^+ , C_6H_4^+ , C_4H_4^+ , C_4H_3^+ , C_4H_2^+ , and C_3H_3^+ corresponding to m/z of 77, 76, 52, 51, 50, and 39, respectively. These fragments are identical to the major fragment ions resulting from the unimolecular decomposition of the benzene ion.⁴⁸

The measured reduced mobility of the $(\text{C}_2\text{H}_2)_3^+$ ion is $11.54 \pm 0.3 \text{ cm}^2 \text{ V}^{-1} \text{ s}^{-1}$, similar to the value measured for the benzene cation ($11.43 \pm 0.4 \text{ cm}^2 \text{ V}^{-1} \text{ s}^{-1}$).^{46,67} The corresponding Ω 's at 300 K for the $(\text{C}_2\text{H}_2)_3^+$ and the benzene ions are 47.4 ± 1.4 and $47.9 \pm 1.4 \text{ \AA}^2$, respectively. To compare with the linear isomers and other possible structures of the C_6H_6^+ ions, Ω 's for 17 C_6H_6^+ isomers were calculated using the trajectory method.⁴⁶ Figure 9 displays the Ω values calculated for the C_6H_6^+ isomers and their relative total energies (with the energy of the benzene ion, the most stable C_6H_6^+ isomer, taken as zero). The C_6H_6^+ isomers can be grouped into three distinct categories identified as covalent cyclic, covalent linear, and branched and noncovalent ion–molecule isomers. The ions in the second and third groups, including all the acyclic isomers, have Ω values sub-

stantially larger than the measured values for the $(\text{C}_2\text{H}_2)_3^+$ and benzene cations. In the first group, other cyclic isomers such as fulvene, 3,4-dimethylenecyclobutene, and benzvalene have Ω values similar to those measured for the $(\text{C}_2\text{H}_2)_3^+$ and benzene cations within experimental uncertainty. However, there are major differences in the CID spectra of the benzene cation and these cyclic isomers.⁴⁶ Therefore, among the cyclic isomers that have collision cross-sections similar to those measured for the $(\text{C}_2\text{H}_2)_3^+$ (Figure 9), only the benzene cation exhibits a fragmentation pattern (including the characteristic C_3H_3^+ fragment) similar to that measured for the $(\text{C}_2\text{H}_2)_3^+$ ion.

Clearly, the combination of ion mobility and fragmentation data provides conclusive evidence that the $(\text{C}_2\text{H}_2)_3^+$ ion formed from the ionization of large neutral acetylene clusters has indeed the structure of the benzene cation.

We are currently studying polymerization reactions in ionized binary clusters of acetylene, cyanoacetylene, and HCN. These intracluster polymerization reactions are expected to provide novel efficient mechanisms for the build-up of polycyclic aromatic hydrocarbon (PAH) ions and heterocyclics. These polymerization reactions can play important roles in the solar nebula and in interstellar chemistry.^{69,70}

5. Polymerization of Gas-Phase Monomers on Nanoparticle Surfaces

We have recently introduced a novel approach to polymerize olefin vapors on the surfaces of metallic and semiconductor nanoparticles.⁴⁷ In this approach (see Figure 10), a free radical initiator such as 2,2'-azobisisobutyronitrile (AIBN) is dissolved in a volatile solvent such as acetone. Selected nanoparticles, prepared separately using the laser vaporization controlled condensation (LVCC) method,⁷¹ are sonicated in the initiator solution for an appropriate time. The solution is placed on a glass substrate where the solvent is gently evaporated, thus resulting in the formation of initiator-coated nanoparticles. The substrate is then heated ($90 \text{ }^\circ\text{C}$) inside a vacuum chamber where an olefin vapor such as styrene is admitted at a controlled flow rate. The olefin vapor is then polymerized by the activated initiator on the nanoparticle surfaces, and the resulting polymers encapsulate the nanoparticles by forming a polymer coating on the surface.

Figure 11 displays TEM and SEM images of the polymer-containing nanoparticles and illustrates the dispersive nature of the nanoparticles embedded in the polystyrene matrix.

We are currently exploring the capabilities of this method in preparing different polymers and copolymers from olefin vapors on the surfaces of selected nanoparticles, nanorods,

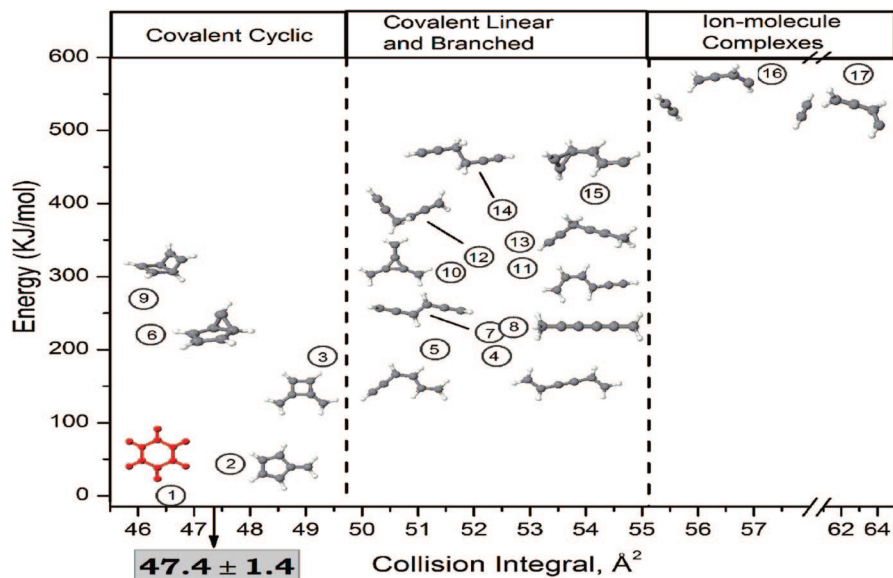


FIGURE 9. Collision integrals and relative energies (relative to the benzene cation) of the $C_6H_6^+$ isomers.

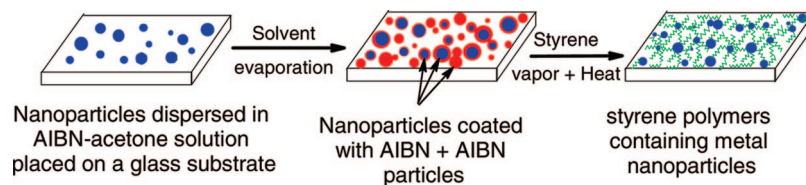


FIGURE 10. Illustration of the approach used to polymerize styrene vapor on nanoparticle surfaces using the free radical initiator 2,2'-azobisisobutyronitrile (AIBN).

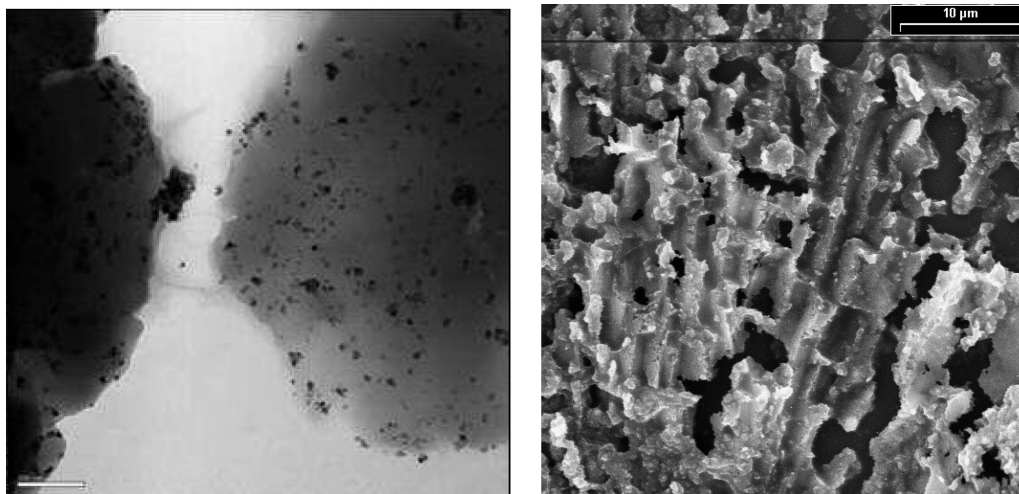


FIGURE 11. TEM (left, scale bar = 200 nm) and SEM (right, scale bar = 10 micron) images of polystyrene-containing Ni and Fe_2O_3 nanoparticles, respectively.

and nanowires characterized by unique electronic, photoluminescent, and magnetic properties. This approach also provides structural and mechanistic information on the early stages of catalyzed gas-phase polymerization through the ion mobility measurements of the gas-phase oligomers. This information can be used to correlate the gas-phase structural properties with the bulk properties and performance of the polymer nanocomposites.

6. Conclusion and Outlook

The gas-phase and cluster polymerization approach provides fundamental insights into the mechanisms of polymerization reactions that are difficult to obtain from condensed-phase studies. This approach extends the capabilities of the state-of-the-art physical chemistry techniques to a multidisciplinary area that has remained relatively unexplored: *polymerization*

in the gas phase, in clusters, and on nanoparticle surfaces. These studies can isolate individual steps in polymerization chains and address representative classes of reactions. The reactions can be characterized in depth, including their overall thermochemistry, potential energy surfaces, energy barriers, and steric/entropic bottlenecks. The structures of the small growing oligomers can be probed and correlated to the polymerization mechanisms. *The overall goal is to develop a molecular level understanding of how specific aspects of the polymerization process (initiation, copolymerization, termination, etc.) can be controlled.* The detailed knowledge of the gas-phase and cluster polymerization mechanisms and structures is important for the rational design and synthesis of controlled nanostructures involving nanoparticle/polymer composites and films. These materials could have unforeseen contributions to chemical and biological sensors, light-emitting devices, and drug delivery.

Many talented graduate students and postdoctoral associates contributed to these studies. Drs. Yezdi Pithawalla (Philip Morris Research Center), Edreese Alsharaeh (George Mason University in UAE), Paul Momoh (LBNL), Yehia Ibrahim (PNNL), and Victor Abdelsayed (Ain Shams University, Cairo, Egypt) are especially acknowledged for their experimental contributions. I also acknowledge the contributions of the collaborations with Dr. M. Mautner (VCU), Dr. Sam Abrash (University of Richmond, VA), and Dr. D. K. Bohme (York University, Canada). This work has been supported by the National Science Foundation (Grant CHE-0414613).

BIOGRAPHICAL INFORMATION

M. Samy El-Shall received his B.S. and M.S. degrees from Cairo University, Egypt, and his Ph.D. degree from Georgetown University. After postdoctoral research with Professors Howard Reiss and R. L. Whetten at UCLA, he joined the Department of Chemistry at Virginia Commonwealth University in 1989, where he is now a Professor of Chemistry and an Affiliate Professor of Chemical Engineering. In 1999, he was awarded the outstanding faculty award of the State Council of Higher Education of Virginia (SCHEV), Virginia's highest faculty honor. His research interests are focused on the chemistry of molecular clusters, gas-phase and cluster polymerization, ion solvation, vapor-phase homogeneous and ion-induced nucleation, synthesis and characterization of nanostructure materials, optical and catalytic properties of nanoparticles, and polymer nanocomposites.

REFERENCES

- Odian, G. *Principles of Polymerization*, 4th ed.; Wiley-Interscience: New York, 2004.
- Faust, R., Shaffer, T. D., Eds. *Cationic Polymerization: Fundamentals and Applications*, ACS Symposium Series 665, American Chemical Society: Washington DC, 1997.

- Matyjaszewski, K., Ed. *Cationic Polymerization: Mechanisms, Synthesis, and Applications*; Marcel Dekker, Inc., New York, 1996.
- Kennedy, J. P.; Ivan, B. *Designed Polymers by Carbocationic Macromolecular Engineering: Theory and Practice*; Hanser: New York, 1992.
- Meot-Ner, M.; Hunter, E. P.; Field, F. H. Thermal and non-thermal decomposition, eliminative ionic polymerization, and negative temperature coefficients in the $i\text{-C}_4\text{H}_{10}$ -benzyl acetate system. *J. Am. Chem. Soc.* **1977**, *99*, 5576–5583.
- Raksit, A. B.; Bohme, D. K. Studies of the initial steps in the polymerization of C_2N_2 induced by Xe^+ . *Can. J. Chem.* **1984**, *62*, 2123–2126.
- Forte, L.; Lien, M. H.; Hopkinson, A. C.; Bohme, D. K. Gas-phase measurements of the kinetics of BF_2^+ -induced polymerization of olefinic monomers. *Can. J. Chem.* **1989**, *67*, 1576–1583.
- El-Shall, M. S.; Marks, C. Cationic polymerization within gas phase clusters of isoprene. *J. Phys. Chem.* **1991**, *95*, 4932–4935.
- El-Shall, M. S.; Schriver, K. E. Observation of eliminative cationic polymerization within van der Waals clusters. *J. Chem. Phys.* **1991**, *95*, 3001–3004.
- Coolbaugh, M. T.; Vaidyanathan, G.; Peifer, W. R.; Garvey, J. F. Cationic polymerization within van der Waals clusters of the form $(\text{CH}_2=\text{R})_n^+$ ($\text{R} = \text{CH}_2$, CF_2 , and CHCH_3). *J. Phys. Chem.* **1991**, *95*, 8337–8343.
- Coolbaugh, M. T.; Whitney, S. G.; Vaidyanathan, G.; Garvey, J. F. Intracuster polymerization reactions within acetylene and methacetylene cluster ions. *J. Phys. Chem.* **1992**, *96*, 9139–9144.
- Wang, J.; Javahery, G.; Petrie, S.; Bohme, D. K. Fullerene dications as initiators of polymerization with 1,3-butadiene in the gas phase: Chemistry directed by electrostatics? *J. Am. Chem. Soc.* **1992**, *114*, 9665–9666.
- Tsukuda, T.; Kondow, T. Anionic polymerization in the gas phase clusters of 2-chloroacrylonitrile. *J. Phys. Chem.* **1992**, *96*, 5671–5673.
- Guo, B. C.; Castleman, A. W., Jr. Dehydration of ethylene and propylene and ethylene polymerization induced by Ti^+ in the gas phase. *J. Am. Chem. Soc.* **1992**, *114*, 6152–6158.
- Daly, G. M.; El-Shall, M. S. Polymerization in clusters and in the gas phase using metal ions. *Z. Phys. D* **1993**, *26S*, 186–188.
- Vann, W.; El-Shall, M. S. Novel approach to cationic polymerization using pulsed laser vaporization/ionization of metals. *J. Am. Chem. Soc.* **1993**, *115*, 4385–4386.
- Brodbeck, J. S.; Liou, C. C.; Maleknia, S.; Lin, T. J.; Lagow, R. J. Reactions of perfluorinated compounds with ethers: Evidence for gas-phase ionic polymerization. *J. Am. Chem. Soc.* **1993**, *115*, 11069–11073.
- Daly, G. M.; El-Shall, M. S. Gas phase reactions between Ti^+ and isobutylene: Cationic polymerization and observation of $\text{C}_4\text{H}_9^+(\text{C}_4\text{H}_8)_n$ by high pressure mass spectrometry. *J. Phys. Chem.* **1994**, *98*, 696–701.
- Wang, J.; Javahery, G.; Petrie, S.; Hopkinson, A. C.; Bohme, D. K. Fullerene dications as initiators for gas-phase “ball-and-chain” polymerization of ethylene oxide: Termination by cyclization. *Angew. Chem., Int. Ed. Engl.* **1994**, *33*, 206–207.
- Tsukuda, T.; Kondow, T. Intracuster anionic polymerization initiated by electron attachment onto olefin clusters $(\text{CH}_2=\text{CXCN})_n$ ($\text{X} = \text{Cl}, \text{H}, \text{D}$, and CH_3) and $(\text{CH}_2=\text{CHC}_6\text{H}_5)_n$. *J. Am. Chem. Soc.* **1994**, *116*, 9555–9564.
- Desai, S. R.; Feigerle, C. S.; Miller, J. Laser induced polymerization within carbon disulfide clusters. *J. Phys. Chem.* **1995**, *99*, 1786–1791.
- Daly, G. M.; El-Shall, M. S. Metal catalyzed polymerization within gas phase clusters: $\text{Al}^+/\text{t-BuCl}/\text{isobutylene}$ system. *J. Phys. Chem.* **1995**, *99*, 5283–5290.
- Daly, G. M.; Pithawalla, Y. B.; Yu, Z.; El-Shall, M. S. Interaction of Zn^+ with isobutylene in the gas phase and in clusters: Metal ion-induced cationic polymerization. *Chem. Phys. Lett.* **1995**, *237*, 97–105.
- Meot-Ner, M.; Sieck, L. W.; El-Shall, M. S.; Daly, G. M. Comparative polymerization in the gas phase and in clusters. 1. Covalent dimer formation and entropy barriers to polymerization in isobutene. *J. Am. Chem. Soc.* **1995**, *117*, 7737–7743.
- El-Shall, M. S.; Daly, G. M.; Yu, Z.; Meot-Ner, M. Comparative polymerization in the gas phase and in clusters. 2. Electron impact and multiphoton induced reactions in isobutene and benzene/isobutene clusters. *J. Am. Chem. Soc.* **1995**, *117*, 7744–7752.
- El-Shall, M. S.; Slack, W. Ultrafine metal particles in polymers and the formation of periodic polymer stripes. *Macromolecules* **1995**, *28*, 8456–8458.
- El-Shall, M. S. Laser ablation for the synthesis of nanoparticles and polymers containing metal particulates. *Appl. Surf. Sci.* **1996**, *106*, 347–355.
- El-Shall, M. S.; Yu, Z. Concerted reactions of charge transfer and covalent bond formation in ionized alkylbenzene-isobutene clusters. Copolymerization of styrene-isobutene and α -methylstyrene-isobutene clusters. *J. Am. Chem. Soc.* **1996**, *118*, 13058–13068.
- Pithawalla, Y. B.; Gao, J.; Yu, Z.; El-Shall, M. S. Even/odd alternation in styrene cluster ions. Evidence for multiple cyclization during the early stages of polymerization and the inhibition effect of water. *Macromolecules* **1996**, *29*, 8558–8561.

- 30 Bjarnason, A.; Ridge, D. P. Pressure dependence of metal-catalyzed polymerization in the gas phase. A study of radiative and collisional relaxation. *J. Phys. Chem.* **1996**, *100*, 15118–15123.
- 31 Zhong, Q.; Poth, L.; Shi, Z.; Ford, J. V.; Castleman, A. W., Jr. Intracluster polymerization reactions of alkene cluster ions. *J. Phys. Chem.* **1997**, *101*, 4203–4208.
- 32 Meot-Ner, M.; Pithawalla, Y. B.; Gao, J.; El-Shall, M. S. Coupled reactions of condensation and charge transfer. 1. Formation of olefin dimer ions in reactions with ionized aromatics. Gas phase studies. *J. Am. Chem. Soc.* **1997**, *119*, 8332–8341.
- 33 Baranov, V.; Wang, J.; Javahery, G.; Hopkinson, A. C.; Bohme, D. K. Fullerene dications and trications as initiators in the gas phase “ball-and-chain” polymerization of allene and propyne: Observation of a remarkable periodicity in chain growth with allene. *J. Am. Chem. Soc.* **1997**, *119*, 2040–2049.
- 34 Pithawalla, Y. B.; El-Shall, M. S. Gas phase and cluster studies of the early stages of cationic polymerization and the reactions with metal cations. In *Solvent-Free Polymerization and Processes*; Hunt, M. O., Long, T. E., Eds.; ACS Symposium Series, American Chemical Society: Washington DC, 1998; Chapter 15, pp 232–245.
- 35 Ohshimo, K.; Misaizu, F.; Ohno, K. Anionic oligomerization of acrylonitrile molecules initiated by intracluster electron transfer from alkali metal atoms: Photoionization mass spectrometry of $M(\text{CH}_2=\text{CHCN})_n$ ($M = \text{Li, Na, and K}$). *J. Phys. Chem. A* **2000**, *104*, 765–770.
- 36 Hiraoka, K.; Sugiyama, T.; Kojima, T.; Katsuragawa, J.; Yamabe, S. A gas-phase polymerization reaction in the cluster ion $\text{NO}^+(\text{propylene})_n$. *Chem. Phys. Lett.* **2001**, *349*, 313–320.
- 37 Tsunoyama, H.; Ohshimo, K.; Misaizu, F.; Ohno, K. Intracluster anionic oligomerization of acrylic ester molecules initiated by electron transfer from an alkali metal atom. *J. Am. Chem. Soc.* **2001**, *123*, 683–690.
- 38 Pithawalla, Y. B.; Meot-Ner, M.; Gao, J.; El-Shall, M. S.; Baranov, V. I.; Bohme, D. K. Gas phase oligomerization of propene initiated by benzene radical cation. *J. Phys. Chem. A* **2001**, *105*, 3908–3916.
- 39 Pithawalla, Y. B.; Gao, J.; El-Shall, M. S. Prospects for the study of gas phase polymerization and the synthesis of polymers containing nanoparticles in microgravity. In *Polymer Processing in Microgravity*; Pojman, J. A., Ed.; ACS Symposium Series, American Chemical Society: Washington DC, 2001; Chapter 13, pp185–202.
- 40 Ohshimo, K.; Furuya, A.; Tsunoyama, H.; Misaizu, F.; Ohno, K. Photoionization mass spectroscopy of clusters of alkali metal atoms with methyl vinyl ketone and acrolein: Intracluster oligomerization initiated by electron transfer from a metal atom. *Int. J. Mass Spectrom.* **2002**, *216*, 29–40.
- 41 Mahmoud, H.; Germanenko, I. N.; Wright, D.; El-Shall, M. S. The chemistry of styrene (water) $_n$ clusters, $n = 1–5$: spectroscopy and structure of the neutral clusters, deprotonation of styrene dimer cation, and implication to the inhibition of cationic polymerization. *J. Phys. Chem. A* **2005**, *109*, 4474–4483.
- 42 Alsharaeh, E. H.; Ibrahim, Y. M.; El-Shall, M. S. Direct evidence for the gas phase thermal polymerization of styrene. Determination of the initiation mechanism and structures of the early oligomers by ion mobility. *J. Am. Chem. Soc.* **2005**, *127*, 6164–6165.
- 43 Abdelsayed, V.; Ibrahim, Y.; Deevi, S.; El-Shall, M. S. Polymerization of butadiene on nanoparticles’ surfaces and formation of metal/polymer nanocomposites. *Appl. Surf. Sci.* **2006**, *252*, 3774–3782.
- 44 Mahmoud, H.; Germanenko, I. N. M. S.; El-Shall, M. S. Early stages of styrene-isoprene copolymerization in gas phase clusters probed by resonance enhanced multiphoton ionization. *J. Phys. Chem. A* **2006**, *110*, 4296–4298.
- 45 Ibrahim, Y. M.; Meot-Ner, M.; El-Shall, M. S. Associative charge transfer reactions. Temperature effects and mechanism of the gas phase polymerization of propene initiated by benzene radical cation. *J. Phys. Chem. A* **2006**, *110*, 8585–8592.
- 46 Momoh, P. O.; Abrash, S. A.; Mabourki, R.; El-Shall, M. S. Polymerization of ionized acetylene clusters into covalent bonded ions. Evidence for the formation of benzene radical cation. *J. Am. Chem. Soc.* **2006**, *128*, 12408–12409.
- 47 Abdelsayed, V.; Alsharaeh, E.; El-Shall, M. S. Catalyzed radical polymerization of styrene vapor on nanoparticle surfaces and the incorporation of metal and metal oxide nanoparticles within polystyrene polymers. *J. Phys. Chem. B* **2006**, *110*, 19100–19103.
- 48 Momoh, P. O.; El-Shall, M. S. Stepwise hydration of ionized acetylene trimer. Further evidence for the formation of benzene radical cation. *Chem. Phys. Lett.* **2007**, *436*, 25–29.
- 49 Bowers, M. T.; Aue, D. H.; Elleman, D. D. Mechanisms of ion–molecule reactions of propene and cyclopropane. *J. Am. Chem. Soc.* **1972**, *94*, 4255–4261.
- 50 Brill, F. W.; Eyley, J. R. Sequential ion–molecule reactions in acetylene. *J. Phys. Chem.* **1981**, *85*, 1091–1094.
- 51 Groenewold, G. S.; Gross, M. Reaction of the vinyl methyl ether cation radical and 1,3-butadiene: A two-step cycloaddition. *J. Am. Chem. Soc.* **1984**, *106*, 6575–6579.
- 52 Buckley, T. J.; Sieck, L. W.; Metz, R.; Lias, S. G.; Liebman, J. F. Consecutive ion/molecule condensation reactions and photodissociation mechanisms of condensation ions in polyacetylenic compounds. *Int. J. Mass Spectrom. Ion Processes* **1985**, *65*, 181–196.
- 53 von Helden, G.; Wyttenbach, T.; Bowers, M. T. Conformation of macromolecules in the gas phase - use of matrix assisted laser desorption methods in ion chromatography. *Science* **1995**, *267*, 1483–1485.
- 54 Scrivens, J. H.; Jackson, A. T.; Yates, H. T.; Green, M. R.; Critchley, G.; Brown, J.; Bateman, R. H.; Bowers, M. T.; Gidden, J. The effect of the variation of cation in the matrix-assisted laser desorption/ionisation-collision induced dissociation (MALDI-CID) spectra of oligomeric systems. *Int. J. Mass Spectrom. Ion Processes* **1997**, *165/166*, 363–375.
- 55 Clemmer, D. E.; Jarrold, M. F. Ion mobility measurements and their applications to clusters and biomolecules. *J. Mass Spectrom.* **1997**, *32*, 577–592.
- 56 Gidden, J.; Jackson, A. T.; Scrivens, J. H.; Bowers, M. T. Gas-phase conformations of synthetic polymers: Poly(methylmethacrylate) oligomers cationized by sodium ions. *Int. J. Mass Spectrom. Ion Processes* **1999**, *188*, 121–130.
- 57 Gidden, J.; Wyttenbach, T.; Jackson, A. T.; Scrivens, J. H.; Bowers, M. T. Gas-phase conformations of synthetic polymers: Poly(ethylene glycol), poly(propylene glycol), and poly(tetramethylene glycol). *J. Am. Chem. Soc.* **2000**, *122*, 4692–4699.
- 58 Gill, A. C.; Jennings, K. R.; Wyttenbach, T.; Bowers, M. T. Conformations of biopolymers in the gas phase: A new mass spectrometric method. *Int. J. Mass Spectrom.* **2000**, *195/196*, 685–697.
- 59 Gidden, J.; Bowers, M. T.; Jackson, A. T.; Scrivens, J. H. Gas-phase conformations of cationized poly(styrene) oligomers. *J. Am. Soc. Mass Spectrom.* **2002**, *13*, 499–505.
- 60 Gidden, J.; Kemper, P. R.; Shammel, E.; Fee, D. P.; Anderson, S.; Bowers, M. T. Applicability of ion mobility to the gas-phase conformational analysis of polyhedral oligomeric silsesquioxanes (POSS). *Int. J. Mass Spectrom.* **2003**, *222*, 63–73.
- 61 Summers, M. A.; Kemper, P. R.; Bushnell, J. E.; Robinson, M. R.; Bazan, G. C.; Bowers, M. T.; Buratto, S. K. Conformation and luminescence of isolated molecular semiconductor molecules. *J. Am. Chem. Soc.* **2003**, *125*, 5199–5203.
- 62 Flory, P. J. The mechanism of vinyl polymerization. *J. Am. Chem. Soc.* **1937**, *59*, 241–253.
- 63 Mayo, F. R. The dimerization of styrene. *J. Am. Chem. Soc.* **1968**, *90*, 1289–1295.
- 64 Chong, Y. K.; Rizzardo, E.; Solomon, D. H. Confirmation of the Mayo mechanism for the initiation of the thermal polymerization of styrene. *J. Am. Chem. Soc.* **1983**, *105*, 7761–7762.
- 65 Kothe, T.; Fischer, H. Formation rate constants of the mayo dimer in the autopolymerization of styrene. *J. Polym. Sci., Part A* **2001**, *39*, 4009–4013.
- 66 Khuong, K. S.; Jones, W. H.; Pryor, W. A.; Houk, K. N. The mechanism of the self-initiated thermal polymerization of styrene. Theoretical solution of a classic problem. *J. Am. Chem. Soc.* **2005**, *127*, 1265–1277.
- 67 Rusyniak, M.; Ibrahim, Y.; Alsharaeh, E.; Meot-Ner, M.; El-Shall, M. S. Mass-selected ion mobility studies of isomerization of the benzene radical cation and binding energy of the benzene dimer cation. Separation of isomeric ions by dimer formation. *J. Phys. Chem. A* **2003**, *107*, 7656–7666.
- 68 Rusyniak, M.; Ibrahim, Y.; Wright, D.; Khanna, S.; El-Shall, M. S. Gas phase ion mobilities and structures of benzene cluster cations $(\text{C}_6\text{H}_6)_n^+$, $n = 2–6$. *J. Am. Chem. Soc.* **2003**, *125*, 12001–12013.
- 69 Brooke, T. Y.; Tokunaga, A. T.; Weaver, H. A.; Crovisier, J.; Bockelee-Morvan, D.; Crisp, D. *Nature* **1996**, *383*, 606–607.
- 70 Cernicharo, J.; Heras, M.; Tielens, A. G. G. M.; Pardo, J. R.; Herpin, F.; Guelin, M.; Waters, L. B. F. M. *Astrophys. J.* **2001**, *546*, L123–L126.
- 71 El-Shall, M. S.; Abdelsayed, V.; Pithawalla, Y. B.; Alsharaeh, E.; Deevi, S. C. Vapor phase growth and assembly of metallic, intermetallic, carbon, and silicon nanoparticle filaments. *J. Phys. Chem. B* **2003**, *107*, 2882–2886.